Available online at www.sciencedirect.com
ScienceDirect
Catalysis Today 128 (2007) 145–152
CATALYSIS TODAY
www.elsevier.com/locate/cattod

Bismuth molybdates model catalysts with controlled crystallinities spin-coated on Si (1 0 0)

A. Klisinska [1], A.-S. Mamede, E.M. Gaigneaux *

Unité de Catalyse et Chimie des Matériaux Divisés, Université Catholique de Louvain, Croix du Sud 2/17, Louvain-la-Neuve B-1348, Belgium

Available online 31 August 2007

Abstract

The possibility of spin-coating crystalline multi-element oxide model catalysts using citrate complexes of Bi^{3+} and Mo^{6+} solutions was studied. The characterization of obtained thin films was performed by XRD, Raman spectroscopy, SEM and XPS. XRD and confocal Raman data indicated that Bi_2O_3–MoO_3 mixed systems behaved as dictated by the composition of the starting solutions, and pure α-$Bi_2Mo_3O_{12}$, β-$Bi_2Mo_2O_9$, and γ-Bi_2MoO_6 phases were obtained without any heterogeneity. XPS confirmed that Bi:Mo ratios at the surface of the films never differed from those in the bulk, namely that of the starting co-solutions. SEM revealed that the thickness of the films could be tuned in the range 40–140 nm via adjustment of the spin-rate (2, 3, or 5 krpm) and the concentration of the precursors solution (0.24 or 0.48 M in Mo), without any disturbance of crystallinity, the Bi:Mo ratio or the homogeneity of the films. Performed studies suggested that spin-coating of mixed citrate complexes appears as a versatile and easy route to prepare homogenous films of multi-element transition metal oxides with controlled formulation and crystalline structure.

Keywords: Mixed transition metal oxides; Thin films; Model catalyst; Spin-coating; Citrate precursors

1. Introduction

Bismuth-molybdate based catalysts are widely used for selective (amm)oxidation processes as selective oxidation of propene to acrolein and acrylonitrile, and the oxidative dehydrogenation (ODH) of butene to butadiene [1–4]. In the Bi_2O_3–MoO_3 mixed systems three distinct phases, α-$Bi_2Mo_3O_{12}$, β-$Bi_2Mo_2O_9$, γ-Bi_2MoO_6, are known to be active as catalysts [5,6]. Therefore, numerous investigations on the preparation, the thermal behaviour and the structural changes of bulk bismuth molybdates in order to identify and stabilize the catalytic active phase, and to correlate their crystal structure to the catalytic performances (activity and/or selectivity), have been reported in the literature [7,8]. Nevertheless, the catalytic performances shown by these phases are not always well understood yet. Moreover, the discussion of differences in catalytic properties in terms of different composition of the bulk, may not reflect the real surface composition. Beside the catalytic application, bismuth molybdates are interesting because of their unique physical properties with other potential technical applications such as ion conductors [9], photoconductors [10], optical materials [11] and gas sensors [12].

Surface sensitive spectroscopies (XPS, confocal Raman), operated in their mapping mode, and scanning probe microscopies (AFM, STM) are very promising tools to investigate structural, superficial and catalytic properties of transition metal oxides materials. However, for the efficient applications of these techniques, only flat, smooth and uniform samples could be used to avoid artefacts, that could be obtained on the pictures of surfaces with expanded topography. Clearly said, the catalysts in the form of powders or even powders aggregated as pellets are not suited for these techniques resulting to poor resolutions. Therefore, catalytic elements deposited on flat supports or supports with regular shapes, with controlled morphologies, composed of one layer of crystals with the thickness of approximately 100 nm appear as suitable model samples for these techniques.

Different methods are nowadays used for the thin film deposition, as thermal evaporation [13], sputtering [14], chemical vapour deposition (CVD) [15], laser deposition

* Corresponding author. Fax: +32 10 473649.
E-mail address: gaigneaux@cata.ucl.ac.be (E.M. Gaigneaux).
[1] On leave from Institute of Catalysis and Surface Chemistry, Polish Academy of Sciences, Krakow, Poland.

0920-5861/$ – see front matter © 2007 Elsevier B.V. All rights reserved.
doi:10.1016/j.cattod.2007.06.068

[16], or flash evaporation [17]. As an alternative, spin-coating appears as a most promising, simple and versatile method for the preparation of the thin films. Spin-coating of amorphous precursors [18] leads, after appropriate calcinations, to transition metal oxide films consisting in regular mosaics of crystals laying flat on the substrate. These uniform and smooth films thus constitute realistic model samples for the corresponding catalytic oxide powders, while being suited for the characterization tools mentioned. However, up to now only mono-metallic oxide films, obtained by the reaction of metals (Mo, V, W) with hydrogen peroxide, were produced through this method [19,20].

A complexation method is an efficient way to homogenously combine several metals in a mixed oxide, resulting in high purity of the obtained solids, and allowing to finely control their structure through optimization of the calcination of amorphous intermediate cakes [21]. The complexation method consists in contacting dissolved precursors of the metals to be combined in a mixed oxide in the presence of a polyfunctional carboxylic acid (oxalic or citric for example). The latter will co-complex, in a giant 3D assembly and in a statistically close proximity the metals. The subsequent gelification of the complex (by removing the water) and afterwards the controlled thermal decomposition of the organic fraction then leads to finely dispersed mixed oxides. Based on that fact the attempt has been made to implement it into the preparation of thin films of multi-element transition metal oxides. There are many suitable organic complexants but citric acid is the most frequently used for preparation of powders [21], in particular Bi molybdate systems [22], thus the ''citrate complexation route'' was applied.

Therefore, the aim of this work is to investigate the possibility to spin-coat thin films of various ''mixed citrate complexes'' of bismuth and molybdenum, and to evaluate the efficiency of such a combination to grow homogenous films of bismuth molybdates with well-defined α, β and γ crystalline forms of interest in catalysis.

2. Experimental

2.1. Thin films preparation

Thin films of bismuth molybdates were deposited by spin-coating on Si tiles exposing the (1 0 0) face. Before deposition Si tiles were cut with a diamond cutter in a liquid to square pieces (0.9 cm × 0.9 cm) and pretreated as follows. First, the tiles were cleaned by a dipping in HF aq. (2%) for 20 s to remove organic impurities from the surface [23]. After several rinsing with water (HPLC grade), the tiles were kept in water until a UV/O_3 treatment [24,25] (Jelight's UVO-Cleaner 42, λ = 254 nm) was applied to obtain a static contact angle nearing 0. Besides the removal of the organic impurities, another effect of the HF treatment is also to remove the native oxide layer. The idea of recreating an oxide layer afterwards by UV/O_3, is to obtain a controlled identical oxide layer for each experiment. This would otherwise not be possible with the native non-controlled native oxide layer.

The precursor solutions to bismuth molybdates were prepared by the complexation of metals using the ''citrate'' method. Two series of solutions were prepared with final Mo concentrations of 0.24 M and 0.48 M (hereinafter notes as ''Conc1'' and ''Conc2''), each series being prepared with three different Bi:Mo molar atomic ratios, namely 2:3, 1:1 and 2:1 (hereinafter noted ''R2:3'', ''R1:1'' and ''R2:1''). Six different solutions were prepared as follows. $(NH_4)_6Mo_7O_{26}{\cdot}4H_2O$ (Aldrich, >99%) and $Bi(NO_3)_2{\cdot}5H_2O$ (Aldrich, 98%) were dissolved separately in distilled water. After their mixture, an aqueous solution of citric acid ($C_6H_8O_7$, Merck, 99.5%) in equivalent amount of 1.5 mol citric acid/mol (Mo + Bi) was added.

Precursor solutions were used for spin-coating immediately after their preparations. The spin-coating deposition was performed in air with a commercial spin-coater from Macronetics. Prior to spinning, Si pieces were covered with several droplets of a precursor solution to form a liquid film completely covering the substrate. Si pieces were spun first at 500 rpm (revolutions per minute) for 3 s, then at 2000 rpm (spin-rate hereinafter noted ''Sp2'') for 60 s, 3500 rpm (''Sp3'') or 5000 rpm (''Sp5'') for 30 s. Newton rings were always observed indicating that evaporation of solvent was completed. Fresh films were then submitted to thermal treatment in air: drying at 140 °C for 1 h followed by calcination at 500 °C for 1 h with heating rate 10° min^{-1} for both cases.

Films thus obtained are denoted as ''R...-Conc...-Sp...'', where ''R...'' indicates the Bi:Mo molecular atomic ratio (R2:3, R1:1, or R2:1), ''Conc...'' shows the concentration of Mo in the precursor solutions (Conc1 = 0.24 M or Conc2 = 0.48 M) and ''Sp...'' presents the spin-rate (Sp2 = 2000 rpm, Sp3 = 3500 rpm or Sp5 = 5000 rpm), respectively.

2.2. Thin films characterization

X-ray diffraction (XRD) was measured in air on a Kristalloflex Siemens D5000 diffractometer using Cu Kα radiation (λ = 1.5418 Å). The 2θ range was scanned from 10 to 70° at a rate of 0.3° min^{-1} with Si pieces laying flat on the sample holder. Laser Raman spectroscopy (LRS) was performed with a Jobin Yvon confocal spectrometer equipped with a He–Ne laser supplying the excitation line at 632.8 nm with a power of 10 mW. Measurements were carried out with a resolution of 5 cm^{-1}. The acquisition time was typically 4 min. The spectrometer was calibrated using the silicium line at 521 cm^{-1}. No thermal degradation because of the beam (focused as a spot of 1 μm in diameter) was observed during the analysis. In addition, the homogeneity of the surface was checked at different spots of the sample. Scanning electron microscopy (SEM) photographs were taken on a LEO 982 GEMINI microscope equipped with a field emission gun operated with 1 kV as accelerating voltage and 70 μA as emission current. Morphology of the films was observed with the Si (1 0 0) faces perpendicularly positioned to the electron beam. We checked that the presented SEM photographs are representative of the whole surface. Thickness was evaluated during SEM measurements by averaging values measured at

different spots of the edges obtained by cleavage of the Si pieces through the centre of their (1 0 0) faces on six samples for the same series. The length measurements were performed with the average deviation ±10 nm by LEO 982 GEMINI software. X-ray photoelectron spectroscopy (XPS) was performed on an Axis Ultra spectrometer from Kratos working with a monochromatic Al Kα radiation (15 kV, 10 mA). No charge compensation was provided. Pass energy for the analyser was 40 eV and the spot size was 700 μm × 300 μm corresponding to a FWHM of 0.92 eV for the Ag $3d_{5/2}$ band of a freshly sputtered silver standard. The binding energies were calibrated by fixing the C–(C, H) contribution of the C 1s adventitious carbon at 284.8 eV. The analyses were based on the following photopeaks: Bi 4f, Mo 3d, Si 2p, C 1s and O 1s. Peaks were considered to be combinations of Gaussian and Lorentzian functions in a 70/30 ratio, working with a linear baseline (following recommendations from the supplier). For the quantification of the elements, sensibility factors provided by the manufacturers were used.

3. Results and discussion

Fig. 1 shows X-ray diffraction patterns of thin films prepared at a fixed Mo concentration (0.24 M: Conc1) with the Bi:Mo ratios that, respectively, correspond to α-, β- and γ-phases: R2:3-Conc1, R1:1-Conc1, R2:1-Conc1, deposited with various spin-coating rates. The peak at 26.4° observed for R2:3-Conc1 and R1:1-Conc1 systems corresponded to the Si substrate. It is clear from XRD pattern that R2:3-Conc1 thin films can be readily identified as a crystalline α-$Bi_2Mo_3O_{12}$ (JCPDS Card No. 21-0103). Well-defined lines at 12.7, 29.2, 31.0, 32.0 and 53.3° corresponding to (1 0 0), (2 2 1), (0 2 3), (2 0 4) and

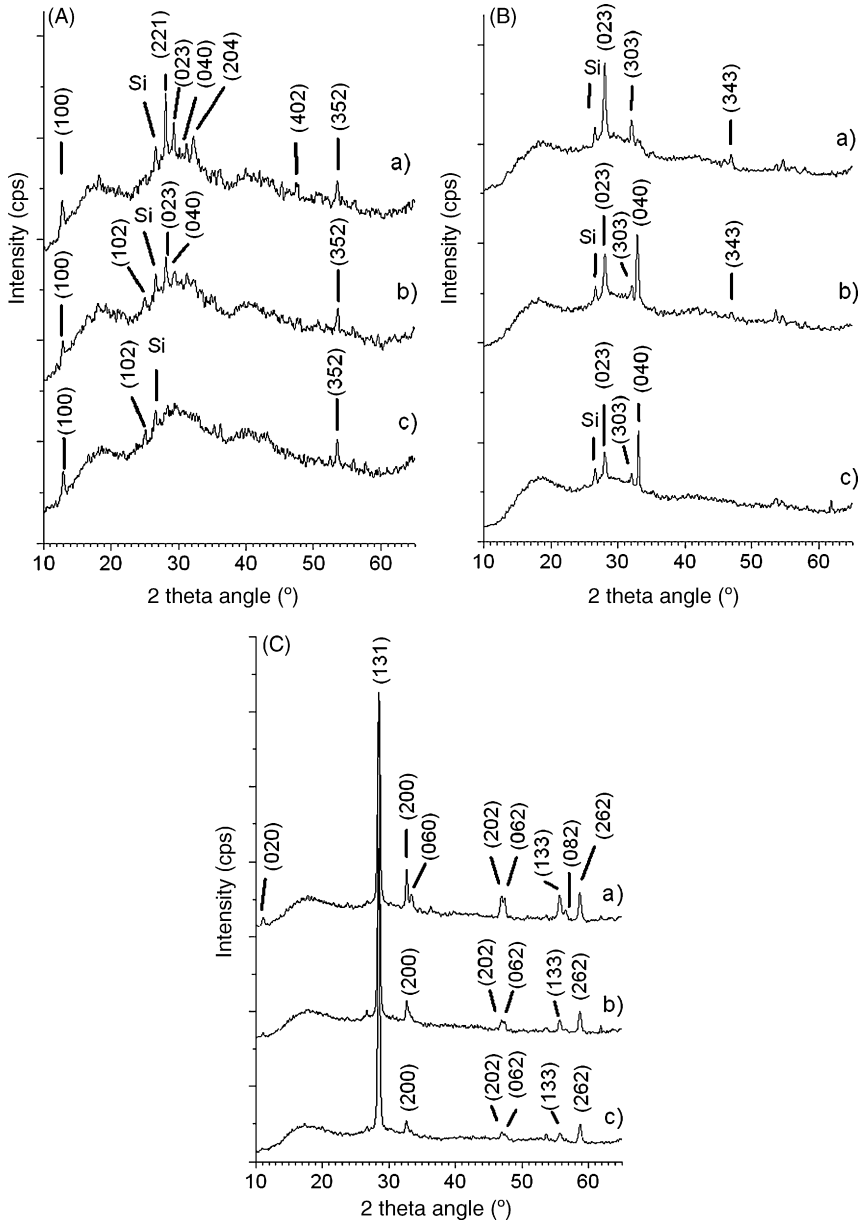

Fig. 1. X-ray diffraction patterns for: (A) R2:3-Conc1; (B) R1:1-Conc1; (C) R2:1-Conc1; at (a) Sp5; (b) Sp3; (c) Sp2.

(3 5 2) planes of α-$Bi_2Mo_3O_{12}$ were observed. The diffraction patterns of R2:3-Conc1 thin films are in close agreement with that reported for the powder α-$Bi_2Mo_3O_{12}$ by Li and Cheng [26] and Ghule et al. [27]. For R1:1-Conc1 thin films, β-$Bi_2Mo_2O_9$ (JCPDS Card No. 33-0209) was identified, as evidenced by peaks at 27.8, 31.8, 33.2 and 46.6° corresponding to (0 2 3), (3 0 3), (0 4 0) and (3 4 3) planes. The XRD pattern of R2:1-Conc1 thin films presents the intensive peak at 28.3° and small peaks at 10.9, 32.5, 33.1, 46.7, 47.1, 55.5, 56.4 and 58.4° corresponding to (1 3 1) and (0 2 0), (2 0 0), (0 6 0), (2 0 2), (0 6 2), (1 3 3), (0 8 2) and (2 6 2) planes, respectively, of γ-Bi_2MoO_6 (JCPDS Card No. 21-0102) phase. The positions of all diffraction lines in R1:1-Conc1 and R2:1-Conc1 samples agreed well with those previously presented by Chen and Smith [28] and Aykan [29] for β-$Bi_2Mo_2O_9$ and γ-Bi_2MoO_6 powders, respectively. The peaks representing MoO_3 were never observed in any studied samples. The differences in the intensities of several diffraction peaks among the samples were further observed. The intensity of peaks increase with the increasing spin-rate. This observation suggests that the crystallinity and microstucture of the deposited thin films were different from each other. One can suspect that for films obtained at the highest spin-coating rate the crystals are bigger, and thus present more crystalline particles. This may at first glance seem somehow paradoxical as films spin-coated at highest spin-rates are those which, on the basis of the spin-coating theory, have the less important deposits. One can thus imagine that films with less matter would be less organized. Our XRD data suggest the opposite. This information will actually be confirmed on the basis of the SEM observations (see after: Figs. 3–5 and Table 1).

As reported in literature [30], pure α-phase can be synthesized for samples having Bi:Mo ratio of 2:3 in the temperature range from 400 to 620 °C. The formation of β-phase in samples having Bi:Mo ratio of 1:1 at low temperatures (300–400 °C) is accompanied with the formation of small amounts of α- and γ-phases, which further react with each other to produce β-phase until 580 °C. The pure γ-phase can be synthesized for samples having Bi:Mo ratio of 2:1 in the range between 500 and 580 °C. Above the latter temperature a non-reconstructive transition of γ-phase into γ′-phase occurs. Considering the calcination temperature of prepared samples, one could have predicted the presence of α-$Bi_2Mo_3O_{12}$, β-$Bi_2Mo_2O_9$, and γ-Bi_2MoO_6 in R2:3-Conc1, R1:1-Conc1 and R2:1-Conc1 thin films, respectively, which is in agreement with presented XRD data.

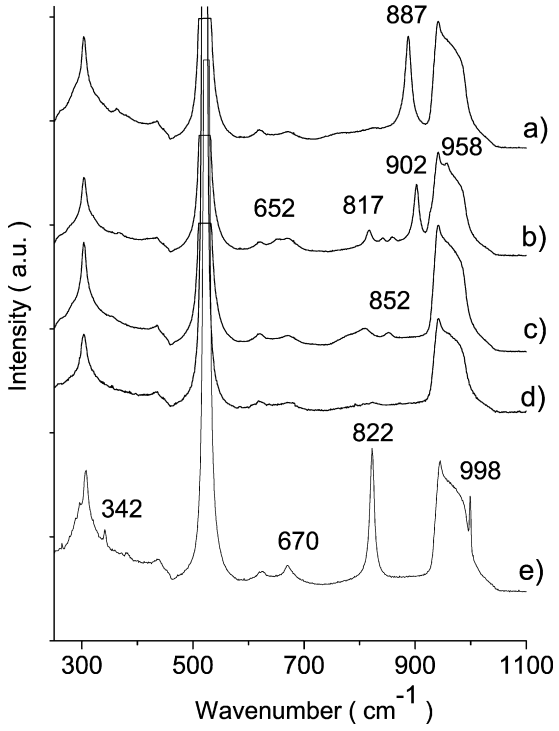

Fig. 2. Laser Raman spectra for: (a) R2:3-Conc1; (b) R1:1-Conc1; (c) R2:1-Conc1; (d) bare Si (1 0 0) wafer; (e) MoO_3 spin-coated on Si (1 0 0).

The Raman spectra of thin films of bismuth molybdates are presented in Fig. 2. The spectrum of bare Si (1 0 0) wafer and thin film of MoO_3 spin-coated on Si (1 0 0) are also given as reference. The intense peak located at 300, 520 cm^{-1} and a broad

Table 1
Main characteristics of the films

Film	Homogeneity			Crystal		Thickness (nm)
	Voids	Size of voids	Percent of voids	Size (nm^2)	Phases detected by XRD	
R2:3-Conc1-Sp2	Yes	250	17	100 × 130	α-$Bi_2Mo_3O_{12}$	70
R2:3-Conc1-Sp3	Yes	500	31	120 × 130	α-$Bi_2Mo_3O_{12}$	70
R2:3-Conc1-Sp5	Yes	1 μm	48	200 × 200	α-$Bi_2Mo_3O_{12}$	40
R2:3-Conc2-Sp2	Yes	200 nm	20	100 × 100	α-$Bi_2Mo_3O_{12}$	120
R2:3-Conc2-Sp3	Yes	300 nm	20	100 × 130	α-$Bi_2Mo_3O_{12}$	90
R2:3-Conc2-Sp5	Yes	600 nm	25	100 × 150	α-$Bi_2Mo_3O_{12}$	60
R1:1-Conc1-Sp2	Yes	300 nm	34	50 × 100	β-$Bi_2Mo_2O_9$	130
R1:1-Conc1-Sp3	Yes	400 nm	48	90 × 100	β-$Bi_2Mo_2O_9$	50
R1:1Conc1-Sp5	Yes	1 μm	79	200 × 200	β-$Bi_2Mo_2O_9$	40
R1:1-Conc2-Sp2	Yes	200 nm	26	50 × 80	β-$Bi_2Mo_2O_9$	140
R1:1-Conc2-Sp3	Yes	200 nm	36	70 × 90	β-$Bi_2Mo_2O_9$	120
R1:1-Conc2-Sp5	Yes	250 nm	47	90 × 100	β-$Bi_2Mo_2O_9$	80
R2:1-Conc1-Sp2	Yes	70 nm	10	70 × 100	γ-Bi_2MoO_6	70
R2:1-Conc1-Sp3	Yes	60 nm	9	80 × 100	γ-Bi_2MoO_6	60
R2:1-Conc1-Sp5	Yes	70 nm	11	80 × 100	γ-Bi_2MoO_6	40

band extending from approximately 930 to 1000 cm^{-1} are observed in all studied systems. These bands are due to the vibrational mode of the silicium substrate [17]. All thin films are free of microcrystalline molybdenum oxide, since no signal at 997 cm^{-1} characteristic for Mo=O stretching mode of terminal oxygen in α-MoO_3 phase was observed. In R2:3-Conc1 thin films, beside the bands of Si substrate, peaks at 652, 817, 842, 861 and 902 cm^{-1} (the most intense), and a shoulder at 958 cm^{-1} were observed. They can be associated with Mo–O stretching vibrations in α-$Bi_2Mo_3O_{12}$, respectively [27,31]. The R1:1-Conc1 systems possess a sharp peak at 887 cm^{-1}, which can be attributed to Mo–O vibrations in β-$Bi_2Mo_2O_9$ [32]. For R2:1-Conc1 samples the presence of γ-Bi_2MoO_6 phase was demonstrated from the occurrence of two peaks at 809 and 852 cm^{-1}. That band is characteristic for the Mo–O–Mo vibration in γ-Bi_2MoO_6. The peaks characteristic for α-Bi_2O_3 (at 298, 319 and 451 cm^{-1}), β-Bi_2O_3 (at 450 and 307 cm^{-1}) and γ-Bi_2O_3 (at 570 cm^{-1}) were not observed in any studied samples [31,33]. The Raman spectra obtained for the thin films of bismuth molybdates coincide with the signals previously reported in the literature for powders [34]. The absence of bands belonging to bulk metal oxides indicated that no segregation of bulk metal oxides occurred during calcination of the mixed metal precursor. The structural features retrieved from the Raman spectra are fully consistent with the information obtained from the XRD patterns.

A selection of SEM pictures for the thin films of α-, β- and γ-phases of bismuth molybdates are presented in Figs. 3–5, respectively. In addition, Table 1 summarizes the main corresponding information. For R2:3-Conc1 and R1:1-Conc1 samples the well-defined crystals are observed. In both cases, the crystal size increase with the increase of the spin-rate. This was already suspected from XRD, and thus confirmed by SEM. The average dimensions of β-$Bi_2Mo_2O_9$ crystals change from 50 nm × 100 nm for R1:1-Conc1-Sp2, to 90 nm × 100 nm for R1:1-Conc1-Sp3, to 200 nm × 200 nm for R1:1-Conc1-Sp5. Similar order is observed for the R2:3-Conc1 series. Furthermore, the thickness of the samples decreases with the increase of the spin-rates. This is in full agreement with theoretical model of spin-coating. The thickness of the films varies in the range 40–130 nm for R2:3-Conc1 and R1:1-Conc1 samples as a function of the spin-rate. With the increase of concentration of the precursor solution a decrease in the crystal size was observed. Thus, for R2:3-Conc1-Sp5 the film was made of crystals with average dimensions of 200 nm × 200 nm, while the crystals of R2:3-Conc2-Sp5 had dimensions of 100 nm × 150 nm. Similarly, for R1:1-Conc1-Sp5 and R1:1-Conc2-Sp5 the crystal size decrease from 200 nm × 200 nm to 90 nm × 100 nm, respectively. The fact that the size of crystallites is larger for thinner films could be explained by the understanding that in general a crystallization proceeds more efficiently when there are less crystal seeds formed in the system – i.e. less germs – making that the available matter crystallizes in less crystals. The latters thus turn bigger and more crystalline. Also, the changes in concentration of α- and

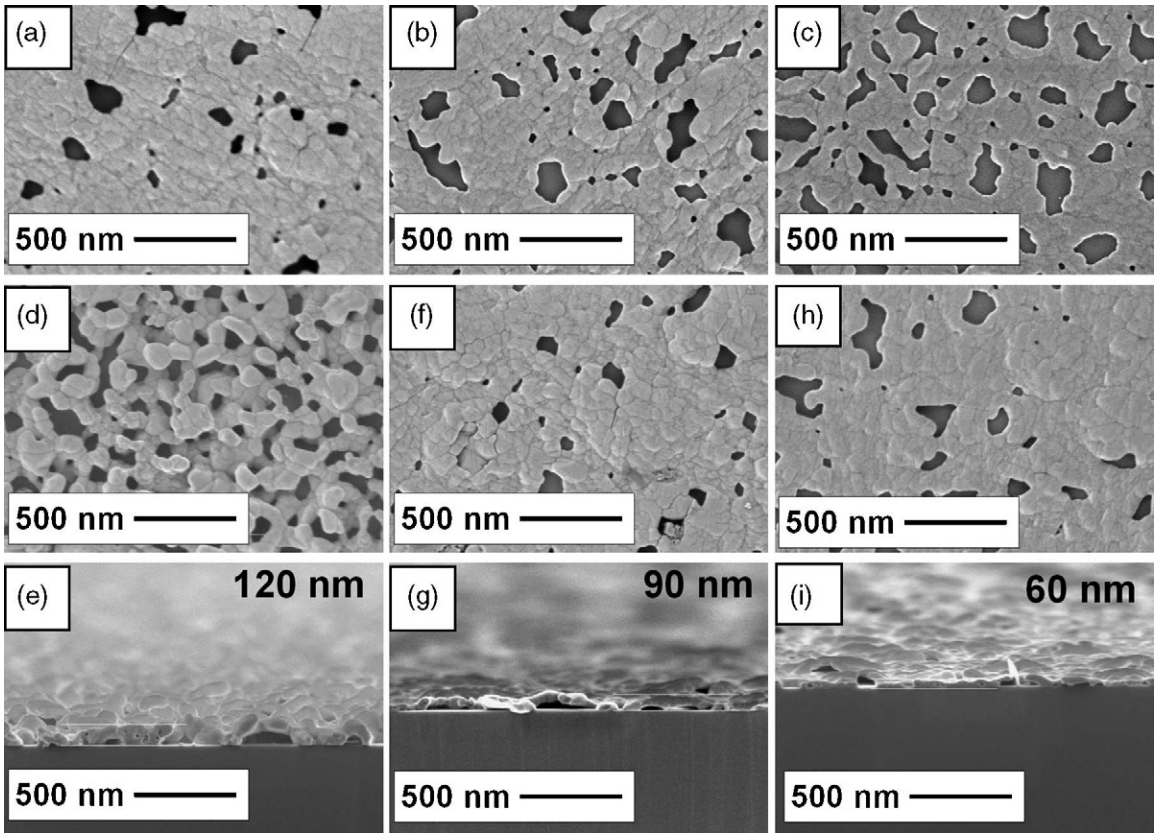

Fig. 3. Scanning electron microscopic (SEM) photographs of: (a) R2:3-Conc1-Sp2; (b) R2:3-Conc1-Sp3; (c) R2:3-Conc1-Sp5; (d) R2:3-Conc2-Sp2; (e) and its edge; (f) R2:3-Conc2-Sp3; (g) and its edge; (h) R2:3-Conc2-Sp5; (i) and its edge.

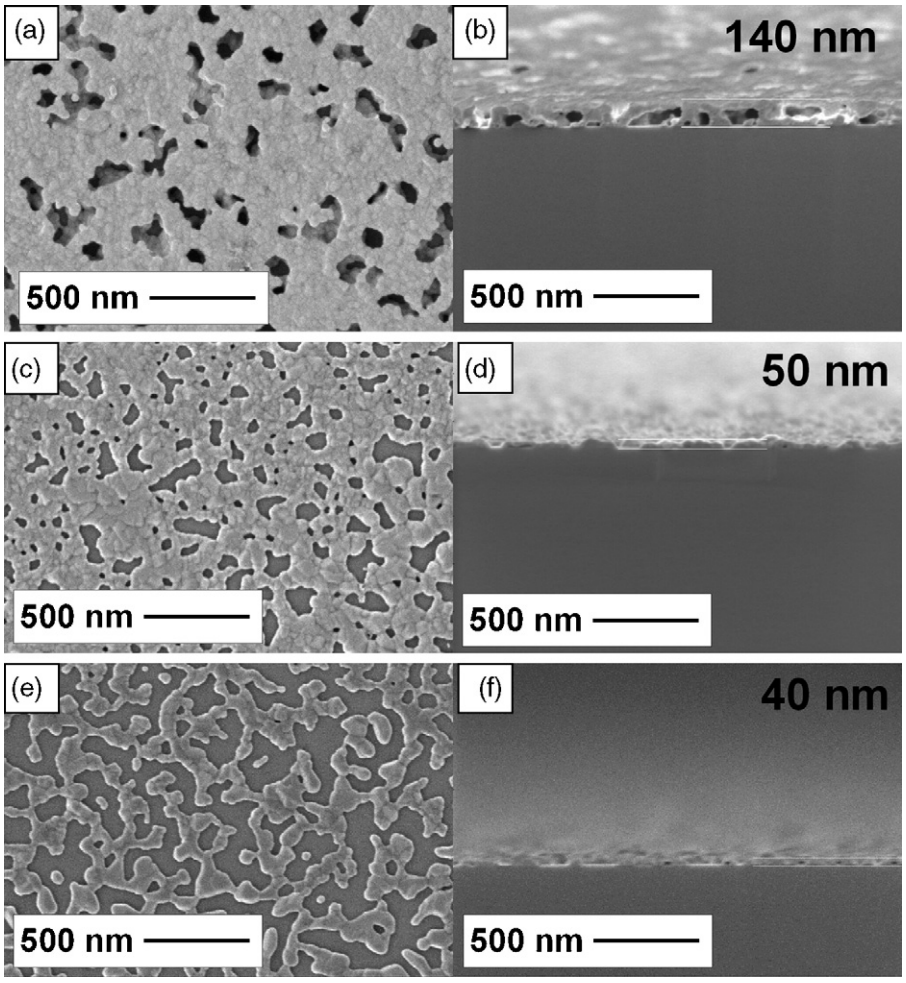

Fig. 4. Scanning electron microscopic (SEM) photographs of: (a) R1:1-Conc1-Sp2; (b) and its edge; (c) R1:1-Conc1-Sp3; (d) and its edge; (e) R1:1-Conc1-Sp5; (f) and its edge.

β-bismuth molybdates precursor solution are connected with the continuity of the samples. For the samples prepared from the solution with the lowest concentration, R2:3-Conc1-Sp3 and R1:1-Conc1-Sp3, the voids between crystals represent approximately 30–50% of the Si substrate. With the increase of the concentration of the precursor solution, the fraction of voids in the samples decreased. This observation suggests that the differences in hydrophobicity of spin-coating solutions may affect the deposition of the material and on the formation of the voids. The higher fraction of voids observed at higher spin-rate could result from the lower hydrophobicity of solutions Conc1 with lower concentration of precursors. The higher spin-rates lead to throwing the precursor solution out the Si tiles during the deposition and/or to the coalescence of wet thin film into drops of solution immediately after deposition, which results in higher fraction of the voids. For R2:1-Conc1 thin films, the Si (1 0 0) substrate is ideally covered by regular seeds. The well-defined grains have average dimensions around ~80 nm × 100 nm. The size of the crystals is practically the same for the different spin-rates. Furthermore, the increase of the spin-rate from 2000 to 5000 rpm has no effect on the fraction of the voids (remaining ~10%). On the other hand, the spin-rate affects the thickness of the films, which as for the previous samples, decreases with the increase of the spin-rate.

The sample composition of thin films was obtained by XPS analysis. The spectrum of Mo 3d and Bi 4f displayed the characteristic Mo $3d_{5/2}$-Mo $3d_{3/2}$ and Bi $4f_{7/2}$-Bi $4f_{5/2}$ doublets caused by the spin orbit splitting. No peaks of other elements beside Bi, Mo, C, Si and O were observed in the wide XPS spectrum (not shown here) indicating the high purity of samples. The Mo $3d_{5/2}$ binding energy ranges between 232.3 and 232.7 eV and it is in line with those reported in the literature for the various bismuth molybdates (231.8–232.7 eV) [35–37]. The binding energy observed for Bi $4f_{7/2}$ ranges between 159.0 and 159.9 eV. In fact, the values of BE characterizing the Bi component lies at higher binding energy with respect to pure Bi_2O_3 (158.6 eV) [38], and they are similar to those reported in literature for α-, β- and γ-bismuth molybdates (159.8–160.0 eV) [39], this observation prompts us to postulate the formation of bismuth molybdate phases, in agreement with the XRD and confocal Raman data described above. In addition, XPS indicated that Bi:Mo ratios in the films never differed from those of the starting co-solutions. Mo/Bi atomic ratios are thus

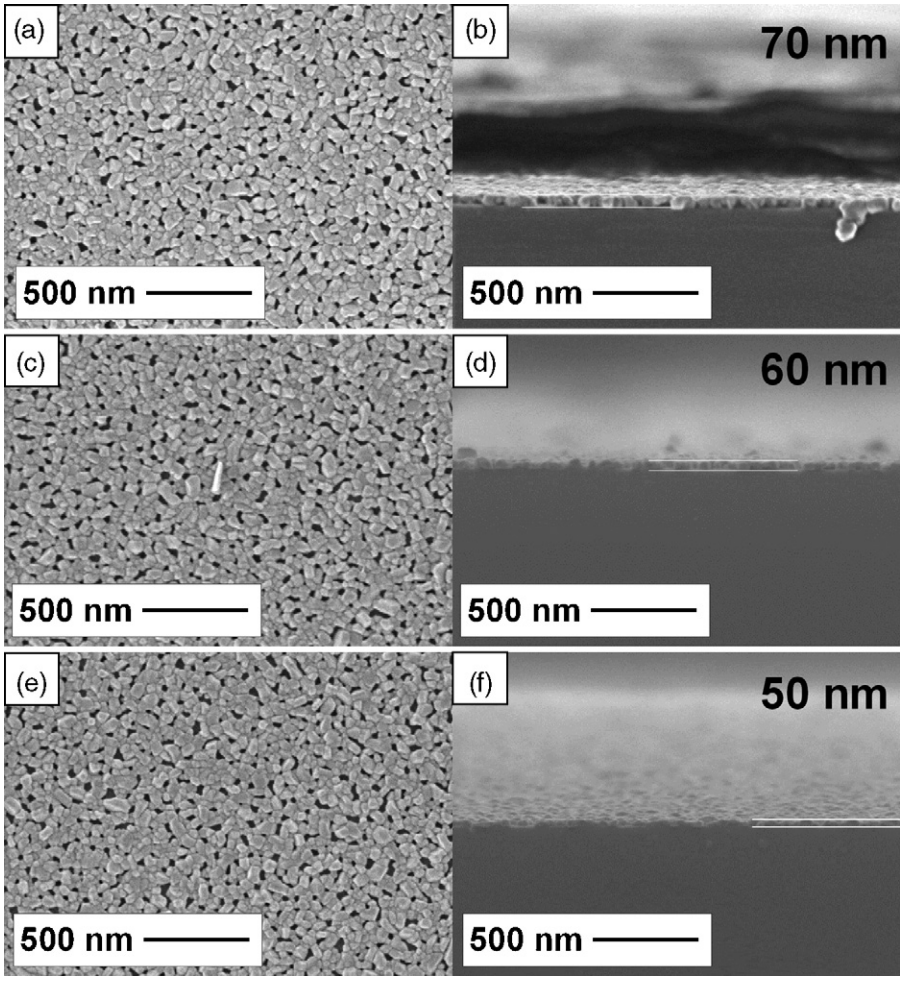

Fig. 5. Scanning electron microscopic (SEM) photographs of: (a) R2:1-Conc1-Sp2; (b) and its edge; (c) R2:1-Conc1-Sp3; (d) and its edge; (e) R2:1-Conc1-Sp5; (f) and its edge.

also similar to those of the bulk for bismuth molybdate catalysts.

4. Conclusions

All characterization data indicated that spin-coated thin films of Bi-systems behaved as expected. XRD proved that the obtained films were made of crystalline α-$Bi_2Mo_3O_{12}$, β-$Bi_2Mo_2O_9$ and γ-Bi_2MoO_6, respectively. Confocal Raman further confirmed that in no case, the films exhibited any heterogenous spots of Bi or Mo simple oxides. XPS confirmed that Bi:Mo ratios in the films never differed from those of the starting co-solutions. SEM revealed that the thickness of the films could be tuned in the range 40–140 nm via adjustment of the spin-rate (2, 3, or 5 krpm) and the concentration of the precursor solution (0.24 or 0.48 M in Mo) without any disturbance of respective crystalline features of the films, their Bi:Mo ratio or continuity.

Performed studies point to spin-coating of mixed citrate complexes as a versatile and easy route to prepare homogenous films of multi-element transition metal oxides with controlled formulation and crystalline structure. The obtained films are suited for surface sensitive spectroscopy and microscopy studies.

Acknowledgements

A.K. thanks the Belgian Federal Science Policy Office for her postdoctoral fellowship. The involvement of the laboratory in the Coordinated Action ‘‘CONCORDE’’ as work package leader; in the Network of Excellence ‘‘FAME’’ of the EU 6th FP, in the IUAP network: ‘‘Supramolecularity’’sustained by the ‘‘Service public fédéral de programmation politique scientifique’’ (Belgium) are also acknowledged.

References

[1] Y. Moro-Oka, W. Ueda, Adv. Catal. 40 (1994) 233.
[2] A.P. Vieira Solares, L.D. Dimitrov, M. Corte-Real Andre de Oliveira, L. Hilaire, M. Farinha Portela, R.K. Grasselli, Appl. Catal. A Gen. 253 (2003) 191.
[3] M.T. Le, W.J.M. Van Well, P. Stoltze, I. Van Driessche, S. Hoste, Appl. Catal. A Gen. 282 (2005) 189.
[4] N. Song, C. Rhodes, J.K. Bartley, S.H. Taylor, D. Chadwick, G.J. Hutchings, J. Catal. 236 (2005) 282.
[5] R.K. Graselli, in: G. Ertl, H. Knőzinger, J. Weitkamp (Eds.), Handbook of Heterogeneous Catalysis, 5, Wiley, New York, 1997, p. 2302.
[6] R.K. Graselli, Top. Catal. 21 (2002) 79.
[7] Z. Bing, S. Pei, S. Shishan, G. Xiexian, J. Chem. Soc. Faraday Trans. 86 (18) (1990) 3145.

[8] H.-G. Lintz, A. Quast, Catal. Lett. 46 (1997) 255.
[9] L.T. Sim, C.K. Lee, A.R. West, J. Mater. Chem. 12 (2002) 17.
[10] T. Sekiya, A. Tsuzuki, Y. Torii, Mater. Res. Bull. 21 (1986) 601.
[11] V. Marinova, M. Veleva, Opt. Mater. 19 (2002) 329.
[12] N. Hykaway, W. Seers, M.R. Frindt, S.R. Morrison, Sens. Actuators 15 (1988) 105.
[13] N. Miyata, T. Suzuki, R. Ohyama, Thin Solid Films 281–282 (1996) 218.
[14] A. Gorenstein, J. Scarminio, A. Lourenc, Solid State Ionics 86–88 (1996) 977.
[15] A. Abdellaoui, G. Leveque, A. Donnadieu, A. Bath, B. Bouchiki, Thin Solid Films 304 (1997) 39.
[16] Z. Geretovszky, T. Szorenyi, Appl. Surf. Sci. 109–110 (1997) 467.
[17] C. Julien, A. Khelfa, O.M. Hussain, G.A. Nazri, J. Cryst. Growth 156 (1995) 235.
[18] E.M. Gaigneaux, K. Fukui, Y. Iwasawa, Thin Solid Films 374 (2000) 49.
[19] K. Yamanaka, H. Oakamoto, H. Kidou, T. Kudo, Jpn. J. Appl. Phys. 25 (1986) 1420.
[20] K. Hinokuma, K. Ogasawara, A. Kishimoto, S. Takano, T. Kudo, Solid State Ionics 53–56 (1992) 507.
[21] P. Courty, H. Ajot, C. Marcilly, B. Delmon, Powder Technol. 7 (1973) 21.
[22] E. Godard, E.M. Gaigneaux, P. Ruiz, B. Delmon, Catal. Today 61 (2000) 279.
[23] H.W. Kim, R. Reif, Thin Solid Films 305 (1997) 280.
[24] J.R. Vig, J. Vac. Sci. Technol. A 3 (1985) 1027.
[25] J. Ruzyllo, G.T. Duranko, A.M. Hoff, J. Electrochem. Soc. 134 (8A) (1987) 2052.
[26] K.T. Li, W.D. Cheng, Appl. Catal. A Gen. 142 (1996) 315.
[27] A.V. Ghule, K.A. Ghule, S.H. Tzing, J.Y. Chang, H. Chang, Y.C. Ling, Chem. Phys. Lett. 383 (2004) 208.
[28] X. Chen, M. Smith, J. Solid State Chem. 13 (1975) 288.
[29] K. Aykan, J. Catal. 12 (1968) 281.
[30] M.T. Le, J.V. Craenenbroeck, I.V. Driessche, S. Hoste, Appl. Catal. A Gen. 249 (2003) 355.
[31] A. Ghule, S. Tzing, J. Chang, K. Ghule, H. Chang, Y. Ling, Eur. J. Inorg. Chem. (2004) 1753.
[32] I. Matsuura, R. Schut, K. Hirakawa, J. Catal. 63 (1980) 152.
[33] L.E. Briand, A.M. Hirt, I.E. Wachs, J. Catal. 202 (2001) 268.
[34] I.E. Wachs, F.D. Hardcastle, J. Phys. Chem. 95 (1991) 10763.
[35] B. Grzybowska, J. Haber, W. Marczewski, L. Ungier, J. Catal. 42 (1976) 327.
[36] I. Matsuura, M.W.J. Wolfs, J. Catal. 37 (1975) 174.
[37] M. Devillers, O. Tirions, L. Cadus, P. Ruiz, B. Delmon, J. Solid State Chem. 126 (1996) 152.
[38] Y. Schuhl, H. Baussart, R. Delobel, M. Le Bras, J. Leroy, L.G. Gengembre, J. Rimblot, J. Chem. Soc. Faraday Trans. I 79 (1983) 2055.
[39] D.A.G. Van Oeffelen, J.H.C. Van Hooff, G.C.A. Schuit, J. Catal. 95 (1985) 84.